Marangoni destabilization on a core-annular film flow due to the presence of surfactant

Hsien-Hung Wei
Department of Chemical Engineering, National Cheng Kung University, Tainan 701, Taiwan

(Received 14 March 2004; accepted 16 September 2004; published online 20 December 2004)

In this paper, the linear stability of a two-fluid, surfactant-laden core-annular flow is asymptotically examined in the thin-annulus limit. The instability of the system is determined by the interplay between interfacial tensions, Marangoni effects and viscosity stratification. A scaling analysis is developed to identify the dominant instability mechanisms in various parameter regimes. With proper scalings, the combined effects of Marangoni forces and viscosity stratification on the leading order stability are examined for both cases in the absence and the presence of the core inertia. For each case, a coupled set of linear evolution equations is derived for the interfacial deflection and the surfactant concentration. In the absence of the core inertia, the system with a more viscous film is always unstable due to the presence of surfactant. When the core fluid is more viscous, the stabilizing effect of the core inertia is compromised by the Marangoni destabilization. The resulting critical Reynolds number, beyond which the instability is completely suppressed by the core inertia, increases with surfactant elasticity. © *2005 American Institute of Physics*.
[DOI: 10.1063/1.1833411]

I. INTRODUCTION

A two-fluid core-annular flow (abbreviated here as "CAF") consists of two immiscible fluids flowing cocurrently in a tube, where one (the annular) fluid wets the tube wall and surrounds the other (core) fluid. This flow system arises in a variety of contexts for modeling processes such as lubricated pipelining,[1] liquid–liquid displacement,[2] enhanced oil recovery,[3] and liquid lining flows in airways.[4] In most CAF applications, the annular fluid layer is much thinner compared to the tube radius. The CAF's in this situation are called core-annular film flows (CAFF's). In this paper, we shall restrict our attention to CAFF's and relevant physical aspects.

The interfacial instability of CAFF's plays a vital role in affecting the efficiencies of processes. For example, in the lung, there is a thin liquid layer coating the interior peripheries of airways. This liquid layer normally contains surfactants that reduce surface tensions for maintaining the integrity of the layer during a breathing cycle. When surfactants are insufficient or malfunctioning as in premature infants with respiratory distress syndrome (RDS), strong surface tension forces amplify the growth of the interface and could cause the liquid to block the pathway of air. Clearly, it is necessary to discourage such surface-tension-induced (capillary) instability for preventing airway occlusion. Liquid-bolus dispersal surfactant replacement therapy (SRT) is a remedy to such surfactant deficiency. In this treatment, liquid is instilled into the lung as a vehicle to deliver exogenous surfactants.[4] Such liquid often forms a liquid plug and leaves a trailing film behind or ahead of the liquid plug. In contrast to airway closure, the formation of liquid plugs, e.g., via breathing rates, is required to be appropriately managed in order to efficiently deliver surfactants through one airway generation to another.

As such, it is important to understand the instability mechanisms of CAFF's because it is often critical to the applications mentioned above. In the absence of surfactant, the dominant effects on the stability of CAFF's are capillarity and viscosity stratification. Capillarity destabilizes (stabilizes) the system when wavelengths of disturbances are longer (shorter) than the undisturbed interfacial circumference. Georgiou *et al.*[5] developed the thin-film asymptotics to analytically examine the combined effects of capillarity and viscosity stratification on the linear stability of a vertical CAFF. With proper scalings, the effect of viscosity stratification can be reflected by the coupling of the core dynamics to the lubricated film flow. For a less viscous annular film with a large interfacial tension, viscosity stratification can linearly stabilize the capillary instability at sufficiently large Reynolds numbers. That is, there exists a window of the stability in the Reynolds number space within which a CAFF is always stable. This result is consistent with the previous CAF study obtained by numerically solving for the full Orr–Sommerfeld equations.[1]

In the weakly nonlinear regime, Frenkel *et al.*[6] and Papageorgiou *et al.*[7] derived the Kuramoto–Sivashinsky equations for describing the interfacial evolutions of CAFF's. The latter work in particular included the nonlocal terms that reflected the coupling of the core dynamics via viscosity stratification. These analyses demonstrated that the capillary instability can be arrested by nonlinear effects. The spatio-temporal interfacial dynamics can exhibit either chaotic or traveling wave motions.

Although the above-mentioned CAFF studies have revealed some basic features of the stability of CAFF's, they are, however, subject to two important restrictions: (i) The annular layer is much thinner compared to the tube radius, and (ii) interfacial displacements are much smaller than the

thickness of the thin annular layer. Some spatio-temporal dynamics cannot be predicted by these studies due to these limitations. Kerchman[8] examined the strongly nonlinear interfacial dynamics of a CAFF by allowing sizes of interfacial disturbances to be comparable to the film thickness. His analysis included the weakly nonlinear analysis as a special case. He demonstrated that the features of the dynamics strongly depended on the capillary number *Ca*, the ratio of viscous to surface tension forces based on the properties of the core fluid. The Kuramoto–Sivashinsky nonlinear saturation of the capillary instability[6,7] was indeed identified for $Ca \ll \varepsilon^2$ (where ε is the ratio of the undisturbed film thickness to the core radius). When ε^2/Ca is sufficiently large, the core-annular arrangement may collapse because the interface could bulge into the core. Kouris and Tsamopoulos[9,10] studied the complete nonlinear problems of CAF's, but without restricting the thin annular fluid or sizes of perturbations. They have confirmed the spatio-temporal dynamics that include bamboo waves or traveling waves observed in the CAFF studies.[7,11] More importantly, some of their findings cannot be predicted by the early works based on the aforementioned restrictions.

Most studies on CAF's were only considered for *clean-interface* systems. The stability of such CAF's is fairly understood. However, when the interface is contaminated by surfactants or surface-active agents, how surfactants affect the stability of CAF's has not been yet fully explored. The central issue herein particularly arises from understanding how surfactants interact with base flows to affect the stability of CAF's, in particular of CAFF's. Rumschitzki[12] and Wei and Rumschitzki[13] have addressed this issue. They showed that the features of the instability with surfactant depended on regimes of the capillary number *Ca*. In the small-*Ca* limit or in the absence of base flows, surfactants partially suppress the capillary instability as in a stationary system with surfactant.[14] In the limit of large *Ca* where base flows are strong or capillary forces are absent, the surfactant distribution is rearranged by the basic interfacial velocity, and the induced Marangoni effects could destabilize the system. For a moderately small *Ca*, surfactant could cause more severe destabilization than the clean-interface capillary instability. These findings have significant implications to CAFF applications. For example, for preventing airway closure in space, one may require applying a sufficiently strong airflow for suppressing the capillary instability.[15] However, an improper choice of surfactant properties or dosages could exaggerate the interfacial growth. In the application of SRT, the flow-induced Marangoni instability could trigger the formation of liquid plugs. But the size of a surfactant-laden liquid plug could become smaller than that of the surfactant-free case.[13] As a result, a plug may be susceptible to be ruptured by blowing airflows.

The Marangoni instability *solely* induced by base flows was first demonstrated by Frenkel and Halpern[16,17] for the linear stability of the two-layer Couette–Poiseuille flow in the presence of an insoluble surfactant. They showed that, in the Stokes-flow limit, surfactant could destabilize the system that is otherwise stable in the absence of surfactant.

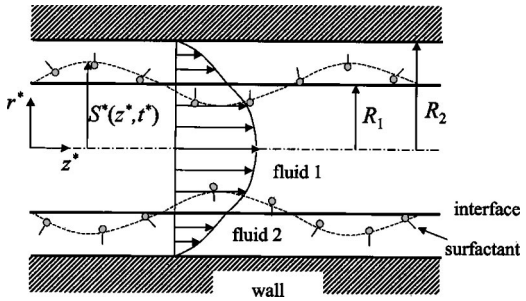

FIG. 1. Geometry of a two-fluid core-annular flow with an insoluble surfactant.

In the study of a surfactant-laden CAFF,[13] the low-*Ca* scaling (i.e., $Ca \sim \varepsilon^2$) demands that the instability is dictated by the film dynamics to which the core dynamics are just slaved. That is, the interaction between surfactant and a base flow is merely through the film dynamics. It is not clear, however, how the inclusion of the core dynamics affects the stability of a CAFF with surfactant. As in the studies of clean-interface CAFF's,[5,7] the contribution from the core flow can enter the analysis when *Ca* is moderately low (i.e., $Ca \sim \varepsilon$). In this regard, there are two issues worth being addressed. First, it has been shown that in the absence of surfactant, a core flow with negligible inertia does not contribute to the instability.[7] This could be changed by the addition of surfactant. Second, in the case inclusive of the core inertia, the stability window in the Reynolds number space could be modified due to the presence of surfactant. In this paper, we shall extend these previous CAFF studies to address the above issues.

II. BASE STATE, GOVERNING EQUATIONS, AND BOUNDARY CONDITIONS

Consider two immiscible, viscous, incompressible fluids flowing axisymmetrically in a core-annular arrangement in a straight tube of radius R_2. See Fig. 1. The interface, defined by $r^* = S^*(z^*, t^*)$, is covered by a monolayer of insoluble surfactant. Fluid 1 of viscosity μ_1 occupies the core region $0 \leqslant r^* \leqslant S^*(z,t)$. Fluid 2 of viscosity μ_2 fills the annular region $S^*(z^*,t^*) \leqslant r^* \leqslant R_2$. Densities of both fluids are matched and denoted by ρ. Because the flow fields are assumed to be axisymmetric, we only consider velocity components $\mathbf{v}^* = (u^*, 0, w^*)$ in terms of the cylindrical coordinates (r^*, θ^*, z^*). Let $r^* = R_1$ be the undisturbed interface. The base flows are driven by a constant pressure gradient $\nabla^* p^* = -F\underline{e}_{z^*}$ with $F > 0$. The characteristic length and velocity are chosen as R_1 and the centerline velocity $W_0 = F(R_1^2(\mu_2 - \mu_1) + R_2^2\mu_1)/4\mu_1\mu_2$, respectively. Pressure is scaled with ρW_0^2 and time has a scale of R_1/W_0. The surface surfactant concentration is scaled with Γ_0^*, an unperturbed, uniform surface concentration associated with the interfacial tension σ_0^*. Define the viscosity ratio $m = \mu_2/\mu_1$ and the radius ratio $a = R_2/R_1$, the base state is

$$\overline{W}(r) = 1 - \frac{mr^2}{(a^2+m-1)} \quad \text{for } 0 \leqslant r \leqslant 1,$$

$$\overline{w}(r) = \frac{(a^2-r^2)}{(a^2+m-1)} \quad \text{for } 1 \leqslant r \leqslant a, \tag{1}$$

$$[\overline{p}] = \frac{1}{Re_1 Ca}, \quad \overline{\Gamma} = 1,$$

where $[\cdot]=(\cdot)_1-(\cdot)_2$. $Re_1=\rho W_0 R_1/\mu_1$ and $Ca=\mu_1 W_0/\sigma_0^*$ denote the Reynolds number and the capillary number, respectively. The nondimensional governing equations for each fluid are

$$\frac{1}{r}(ru)_r + w_z = 0, \tag{2}$$

$$w_t + uw_r + ww_z = -p_z + \frac{1}{Re_i}\nabla^2 w, \tag{3a}$$

$$u_t + uu_r + wu_z = -p_r + \frac{1}{Re_i}\left(\nabla^2 u - \frac{1}{r^2}u\right). \tag{3b}$$

The Reynolds numbers are given by $Re_i=Re_1/m_i$ with $m_1=1$ and $m_2=m$ for $i=1,2$. The system is subject to the following boundary conditions. The velocities vanish on the wall:

$$w_2 = u_2 = 0 \text{ at } r = a. \tag{4}$$

Velocities are continuous at the interface:

$$[w] = 0, [u] = 0 \text{ on } r = S(z,t). \tag{5}$$

The tangential stress and normal stress conditions at the interface $r=S(z,t)$ are given by

$$\frac{1}{(1+S_z^2)}\left[\frac{1}{Re}(w_r+u_z)(1-S_z^2) + \frac{2}{Re}(u_r-w_z)S_z\right] = \frac{1}{CaRe_1}\sigma_z, \tag{6}$$

$$-\left[p - \frac{2}{Re}u_r - \left(-p + \frac{2}{Re}w_z\right)S_z^2 + \frac{2}{Re}(u_r+w_z)S_z\right] = \frac{\sigma(\Gamma)}{CaRe_1}\left[S_{zz} - \frac{1}{S}(1+S_z^2)\right](1+S_z^2)^{-3/2}. \tag{7}$$

The equation of state is assumed to be linear:

$$\sigma = 1 - El(\Gamma - 1), \tag{8}$$

where $El=-(\Gamma_0^*/\sigma_0^*)(\partial\sigma^*/\partial\Gamma^*)_{\Gamma_0^*}$ denotes the elasticity number of surfactant, an ability to lower the interfacial tension in response to surface impurities. The kinematic condition is

$$u = S_t + wS_z \text{ on } r = S(z,t). \tag{9}$$

Finally, for an insoluble surfactant with negligible surface diffusion, the surfactant transport equation along the interface is[18]

$$\Gamma_t - \frac{S_t S_z}{1+S_z^2}\Gamma_z + \frac{1}{S\sqrt{1+S_z^2}}\left(\frac{S(w+uS_z)}{\sqrt{1+S_z^2}}\Gamma\right)_z + \frac{(u-wS_z)}{(1+S_z^2)^2}\left(\frac{1+S_z^2}{S} - S_{zz}\right)\Gamma = 0. \tag{10}$$

III. SCALING ANALYSIS

With the base state as above, we now begin to analyze the corresponding linear stability. Our aim is to asymptotically examine the stability in the thin-annulus limit. To derive the leading order linear stability equations, our strategy essentially follows the previous CAFF studies.[5,7,13] We shall first perform the scaling analysis to identify the dominant instability mechanisms and to estimate the scales of perturbation quantities. We then expand governing equations and boundary conditions with these perturbation quantities to derive the leading order linear stability equations. Since the early asymptotic analysis for a clean-interface CAFF[5] has been justified by comparison with the study obtained from directly solving for the Orr–Sommerfeld equations,[1] we believe that the present asymptotic analysis should capture some essential features that are expected to be found in the full analysis.

Let ε be the ratio of the undisturbed annular thickness to the core radius. The thin-film limit ($\varepsilon \ll 1$) allows one to introduce a stretched film variable $y=1-(r-1)/\varepsilon$ to separate the radial scales in the film and the core. For $m=O(1)$, the leading order base flows are $\overline{w}=2\varepsilon y/m$ and $\overline{W}=1-r^2$ for the film and the core, respectively. Let us introduce infinitesimal disturbances of size $\delta_1(\ll\varepsilon)$ and $\delta_2(\ll 1)$ to the unperturbed interface and surface concentration, respectively:

$$S(z,t) = 1 + \delta_1 \eta(z,t), \tag{11a}$$

$$\Gamma(z,t) = 1 + \delta_2 G(z,t). \tag{11b}$$

Prior to proceeding any further, we have to recognize the fact that the mechanisms of driving perturbed flows can be derived from different routes. For a strong tension or low *Ca*, when the annulus is thin, capillarity due to an interfacial perturbation usually furnishes a large perturbed pressure to drive the film flow. In addition, Marangoni forces generated by the perturbed surfactant distribution also can exert on the interface to induce a flow. This scenario can occur when the tension is weak (i.e., high *Ca*). In this case, the Marangoni-driven mechanism dominates the instability.

To estimate the scales of perturbation quantities, let (w'',u'',p'') and (W'',U'',P'') denote the perturbation quantities for the annulus and the core, respectively. We begin with the capillary scaling for the perturbed film flow and check the consistency *a posteriori*. The perturbed film pressure estimated from the normal stress condition (7) is $p'' \sim \delta_1/Re_1 Ca$. The equation of motions (3) and continuity (2) in the film yield $w'' \sim \varepsilon^2\delta_1/Ca$ and $u'' \sim \varepsilon^3\delta_1/Ca$. As for the core quantities, the continuity of axial velocities across the interface (5) results in $W'' \sim \delta_1$. The lack of separation between the axial and radial length scales demands $U'' \sim \delta_1$ and $P'' \sim \delta_1/Re_1$. The key to including both the core and Ma-

rangoni effects at the leading order lies in the tangential stress condition (6). It requires $Ca \sim \varepsilon$ in view of balancing both the film and core shear stresses at the leading order.[7] This leads the film quantities to $p' \sim \delta_1/\varepsilon Re_1$, $w'' \sim \varepsilon\delta_1$ and $u'' \sim \varepsilon^2\delta_1$. Balancing the viscous shear stresses and the Marangoni stress yields $\delta_1 \sim \delta_2 Ma$ where $Ma = El/Ca$ is the Marangoni number. To gain further information about δ_1, δ_2, Ma and the time scale, we examine the kinematic condition (9) and the surfactant transport equation (10). In a traveling frame with the speed of the basic interfacial velocity, viz. $z \to z - \overline{w}(1)t$, it is necessary to introduce a slow time scale $\tau = \varepsilon^2 t$ to (9) in order to obtain nontrivial dynamics of the perturbed interface. To show more clearly how to derive the relevant surfactant equation and scalings, we first write the linearized form of (10) in terms of unscaled perturbation quantities in the *fixed* coordinate:

$$\Gamma'_t + \overline{w}(y=1)\Gamma'_z + \overline{w_r}|_{r=1}\eta'_z\overline{\Gamma} + w''_z(y=1)\overline{\Gamma} + (u' - \overline{w}\eta'_z)_{y=1}\overline{\Gamma} = 0, \tag{12}$$

where $\eta' \equiv \delta_1\eta$ and $\Gamma' \equiv \delta_2 G$ are the unscaled interfacial perturbation and surfactant disturbance, respectively. We have retained $\overline{\Gamma}$ (=1) here to expedite interpretation of the terms. Notice that $\overline{w} = (2\varepsilon/m)y$ and $\overline{w_r} = -2/m$ have different orders of magnitude. The first term of (12) is the local time rate of change of the surfactant concentration. The other terms except the last term all derive from the surface convection. The second term $[O(\varepsilon\delta_1)]$ is a typical traveling term due to the basic interfacial velocity and clearly has no impact on the stability. The third term $[O(\delta_1)]$ reflects the effect due to the perturbation of the basic interfacial velocity $\overline{w_r}|_{r=1}\eta'$, and the fourth term $[O(\varepsilon\delta_1)]$ derives from the perturbed axial velocity w''. The last term $[O(\varepsilon\delta_1)]$ is attributed to the surface expansion–contraction of the interface. Hence, at the leading order, (12) can be rewritten, in the moving frame of $z \to z - \overline{w}(1)t$, as

$$\varepsilon^2\delta_2 G_\tau - \frac{2}{m}\delta_1\eta_z\overline{\Gamma} = O(\varepsilon\delta_1). \tag{13}$$

Here we have invoked the same long time scale $\tau = \varepsilon^2 t$ used in the kinematic condition. Consequently, a proper scaling relation between δ_1 and δ_2 should come from balancing the first two terms in (13), which yields $\delta_1 \sim \varepsilon^2\delta_2$. This together with the earlier scaling $\delta_1 \sim \delta_2 Ma$ from (6) gives $Ma \sim \varepsilon^2$. In short, the scaling constraints for engaging both surfactant effects and the core dynamics are

$$Ca \sim \varepsilon,\ Ma \sim \varepsilon^2 \text{ and } \delta_1 \sim \varepsilon^2\delta_2. \tag{14}$$

With the above scalings, the perturbed film pressure arising from the surface tension variation due to surfactant is $p'' \sim \delta_2 El/Re_1 Ca \sim \delta_1/Re_1$ which is of a higher order than the capillary pressure $p'' \sim \delta_1/\varepsilon Re_1$. Since the current study is focused on the *linear* stability analysis, sizes of disturbances, in fact, must be *infinitesimal* regardless of ε. Nevertheless, the constraints $\delta_1 \ll \varepsilon \ll 1$ and $\delta_2 \ll 1$ must be at least satisfied here. The scaling $\delta_1 \sim \varepsilon^2\delta_2$ leads to $\delta_1 \ll \varepsilon^2$ which is also reasonable for the linear stability analysis.

Further comments should be made on the scalings (14). $Ca \sim \varepsilon$ is first derived from the capillary scaling for retaining the core dynamics. To recruit Marangoni effects has to further demand $Ma \sim \varepsilon^2$. Since $El = MaCa$, one requires rather diluted surfactant contamination or small surfactant elasticity. In fact, as we shall show next, the analysis for including both Marangoni effects and the core dynamics only requires $Ma \sim \varepsilon^2$ and $\delta_1 \sim \varepsilon^2\delta_2$. It thus can be extended to the regimes beyond $Ca \sim \varepsilon$. In that case, it may not require El to be very small.

For $Ca \gg \varepsilon$, Marangoni forces can drive the film flow at the first place instead of capillary forces. In this case, the perturbed film flow has $w'' \sim \varepsilon\delta_2 Ma$ and $u'' \sim \varepsilon^2\delta_2 Ma$. Balancing the Marangoni-driven film stress and the core stress of (6) yields $\delta_2 Ma \sim \delta_1$. This leads the kinematic condition (9) to have the same long time scale $\tau = \varepsilon^2 t$ as the $Ca \sim \varepsilon$ case. Applying this time scale to the surfactant transport equation (10) yields $\varepsilon^2\delta_2 \sim \delta_1$. With $\delta_2 Ma \sim \delta_1$, we obtain $Ma \sim \varepsilon^2$ and again arrive at the same scaling conditions as (14) except $Ca \sim \varepsilon$. With the scalings $Ma \sim \varepsilon^2$ and $\delta_1 \sim \varepsilon^2\delta_2$, the perturbed film velocities are $w'' \sim \varepsilon\delta_2 Ma \sim \varepsilon\delta_1$ and $u'' \sim \varepsilon^2\delta_1$. Inspecting the capillary scales for the film velocities reveals that for $Ca \gg \varepsilon$, $w'' \sim \varepsilon^2\delta_1/Ca \ll \varepsilon\delta_1$ and $u'' \sim \varepsilon^3\delta_1/Ca \ll \varepsilon^2\delta_1$, indicating that Marangoni effects dominate the instability of the film and the capillary instability is of a higher order effect. All of the perturbed core quantities retain the same scales as earlier regardless of the scale of Ca.

As such, as long as $Ca \gtrsim \varepsilon$, the scalings $Ma \sim \varepsilon^2$ and $\delta_1 \sim \varepsilon^2\delta_2$ of (14) are sufficient to ensure the retaining of both the core and Marangoni effects at the leading order in ε. This is because the perturbed flows can be solely driven by Marangoni stresses without necessarily having capillary forces. Since Ca could be much larger than ε, the required surfactant elasticity $El = MaCa$ is not necessarily small. This scenario in practice could occur in oil recovery processes wherein surfactants are used to reduce interfacial tensions to the ultralow level of 10^{-5}–10^{-3} dyne/cm.[19] For $\mu_1 = 0.01$ poise and the slug's speed of 1 cm/s, $Ca = O(10) - O(10^3)$ which ranges from $O(\varepsilon^{-1})$ to $O(\varepsilon^{-3})$ for $\varepsilon = 0.1$. Therefore, El can span a wide range from $O(\varepsilon)$ to $O(\varepsilon^{-1})$.

The above discussion is for the regime of $Ca \gtrsim \varepsilon$ and $Ma \sim \varepsilon^2$. For other parameter regimes, the dominant mechanisms of instability can differ from the above mentioned. If $Ma \gg \varepsilon^2$, applying similar scaling procedures to a Marangoni-driven flow leads to the time scale $\tau = \varepsilon Ma^{1/2} t$ and the scaling $\delta_1 \sim \varepsilon Ma^{1/2}\delta_2$. Now inspecting the scale of w'' reveals that $w'' \sim \varepsilon\delta_2 Ma \sim \delta_1 Ma^{1/2}$ for the Marangoni scale, and $w'' \sim \varepsilon^2\delta_1/Ca$ for the capillary scale. Accordingly, $Ma^{1/2}Ca/\varepsilon^2$ ($\gg Ca/\varepsilon$ because of $Ma \gg \varepsilon^2$) indicates the relative importance of Marangoni to capillary effects. As a result, for $Ma \gg \varepsilon^2$, when $Ca \gtrsim \varepsilon$, Marangoni effects dominate the instability. On the other hand, if $Ca \ll \varepsilon$ (e.g., $Ca \sim \varepsilon^2$), Marangoni forces are not comparable to capillary forces until $Ma \sim \varepsilon^4/Ca^2$. Since the core shear stress is $O(\delta_1)$ and of a higher order than the film $O(\delta_1 Ma^{1/2}/\varepsilon)$, the system's instability is dictated by the film dynamics to which the core dynamics are slaved. This film-determined instability with surfactant has been identified by Wei and Rumschitzki.[13] The

TABLE I. Dominant mechanisms in various parameter regimes.

	$Ma\sim\varepsilon^2$	$Ma\gg\varepsilon^2$
$Ca\gtrsim\varepsilon$	Capillary-Marangoni instability; the core dynamics are included	Film-determined instability; Marangoni effect dominates
$Ca\ll\varepsilon$	Film-determined instability; capillarity dominates	Film-determined instability; Marangoni effect is not comparable to capillarity until $Ma\sim\varepsilon^4/Ca^2$

above discussion for various parameter regimes is also summarized in Table I.

In the following section for the detailed formulation of the linear stability, we shall focus on the capillary-Marangoni system that satisfies the scaling conditions (14). The case of $Ca\gg\varepsilon$ can be regarded as the weak tension limit of that system.

IV. FORMULATION OF THE LEADING ORDER LINEAR STABILITY

With the scalings (14), the leading order linear stability problem is formulated below. Let $Ca=\varepsilon Ca_0$ and $Ma=\varepsilon^2 M_0$ with $O(1)$ Ca_0 and M_0. The film quantities can be expanded as

$$w=\overline{w}+\varepsilon\delta_1 w'+O(\varepsilon^2\delta_1),$$

$$u=\varepsilon^2\delta_1 u'+O(\varepsilon^3\delta_1), \tag{15a}$$

$$p=\overline{p}+(\delta_1/\varepsilon Re_1)p'+O(\delta_1/Re_1).$$

For the core,

$$W=\overline{W}+\delta_1 W'+O(\varepsilon\delta_1),$$

$$U=\delta_1 U'+O(\varepsilon\delta_1), \tag{15b}$$

$$P=\overline{P}+(\delta_1/Re_1)P'+O(\varepsilon\delta_1/Re_1).$$

After substituting the above into (2)–(10) and expanding them with respect to the base state, the leading order governing equations of the film become

$$u_y'=w_z', \tag{16a}$$

$$0=-p_z'+mw_{yy}', \tag{16b}$$

$$0=-p_y'. \tag{16c}$$

The no-slip conditions $w'(y=0)=u'(y=0)=0$ are applied on the wall. The leading order tangential and normal stress conditions at the interface are given by

$$mw_y'(y=1)=-(W_r'+U_z')_{r=1}-M_0G_z, \tag{17}$$

$$p'=\frac{1}{Ca_0}(\eta+\eta_{zz}). \tag{18}$$

At the leading order, the continuity of velocities at the interface is

$$W'(r=1)=2\left(1-\frac{1}{m}\right)\eta, \tag{19a}$$

$$U'(r=1)=0. \tag{19b}$$

The leading order kinematic condition and surfactant transport equation, in the traveling frame with the basic interfacial velocity $\overline{w}(y=1)$, become

$$u'=\eta_\tau, \tag{20}$$

$$G_\tau-\frac{2}{m}\eta_z=0. \tag{21}$$

Here we have introduced a long time scale $\tau=\varepsilon^2 t$. Notice again that for $Ma\sim\varepsilon^2$ the surface convection due to the perturbed basic interfacial velocity dominates the leading order surfactant transport (21). Further notice that $Ma\sim\varepsilon^2$ admits the absence of the immobilizing effect on the interface due to large surfactant elasticity.

Finally, the leading order governing equations for the core are

$$\frac{1}{r}(rU')_r+W_z'=0, \tag{22a}$$

$$Re_1(-2rU'+(1-r^2)W_z')=-P_z'+\nabla^2 W', \tag{22b}$$

$$Re_1(1-r^2)U_z'=-P_r'+\left(\nabla^2 U'-\frac{U'}{r^2}\right). \tag{22c}$$

The core dynamics that satisfy (19a) and (19b) can be either expressed in terms of the modified Bessel functions for $Re_1=O(\varepsilon)$ (i.e., Stokes flow), or represented by the Kummer functions for $Re_1=O(1)$. The detailed derivations for the core dynamics can be found in the work of Papageoriou *et al.*[7] The film flow field is first determined by using the no-slip conditions, (17) and (18). We then apply this film flow to (20) and (21) for deriving the evolution equations for the interfacial disturbance and the surfactant concentration perturbation, respectively. As a result, the interfacial evolution equation for the $Re_1=O(\varepsilon)$ core flow is

$$\eta_\tau+\frac{1}{3mCa_0}(\eta_{zz}+\eta_{zzzz})+\frac{M_0}{2m}G_{zz}+\frac{i}{\pi m}\left(1-\frac{1}{m}\right)\int_{-\infty}^{\infty}N_B(k)\int_{-\infty}^{\infty}\eta(x,\tau)e^{ik(z-x)}dxdk=0, \tag{23}$$

where

$$N_B(k)=\frac{k^2I_1^2(k)}{kI_1^2(k)-kI_0^2(k)+2I_0(k)I_1(k)},$$

and the function I's and K's are the modified Bessel functions of various orders.

For $Re_1=O(1)$, the corresponding interfacial evolution equation becomes

$$\eta_\tau + \frac{1}{3mCa_0}(\eta_{zz} + \eta_{zzzz}) + \frac{M_0}{2m}G_{zz} - \frac{i}{2\pi m}\left(1 - \frac{1}{m}\right)\int_{-\infty}^{\infty} N_K(k)\int_{-\infty}^{\infty}\eta(x,\tau)e^{ik(z-x)}dxdk = 0, \tag{24}$$

where

$$N_K(k) = \frac{I_1(k)e^{-\lambda}M(\Lambda,2,2\lambda)}{N_1(k)I_0(k) - N_2(k)I_1(k)},$$

with

$$\lambda = \tfrac{1}{2}(kRe_1)^{1/2}e^{-i\pi/4},\ \Lambda = 1 + k^2/8\lambda - \lambda/2,$$

$$N_1(k) = \int_0^1 (I_1(k)K_1(ks) - I_1(ks)K_1(k))s^2e^{-\lambda s^2}M(\Lambda,2,2\lambda s^2)ds,$$

$$N_2(k) = \int_0^1 (I_0(k)K_1(ks) + I_1(ks)K_0(k))s^2e^{-\lambda s^2}M(\Lambda,2,2\lambda s^2)ds,$$

and $M(\Lambda,2,x)$ is the confluent hypergeometric function (the Kummer function).

Notice that our theory is based on lubrication in the film, which requires that the radial length scale in the annulus is much shorter than the axial scale. The analysis is only valid for disturbance wavelengths that are much larger compared to ε. In addition, $Re_1\varepsilon^3/m \ll 1$ is also required for ensuring the validity of lubrication in the film.

V. RESULTS OF THE LEADING ORDER LINEAR STABILITY

For the linear stability analysis, we apply normal modes: $(\eta, G) = (\hat{\eta}, \hat{G})e^{ikz+s\tau}$ to the derived sets of the evolution equations where k ($\ll\varepsilon^{-1}$) is the wave number of the disturbance and s is the complex growth rate. The system's stability is determined by the real part of s, s_r. The system is stable (unstable) when $s_r < 0 (>0)$. Both $Re_1 = O(\varepsilon)$ and $Re_1 = O(1)$ cases are examined separately as below.

A. The $Re_1 = O(\varepsilon)$ case

For $Re_1 = O(\varepsilon)$ or Stokes flow, Eqs. (21) and (23) govern the leading order instability. The dispersion equation for s, after taking normal modes and eliminating $\hat{G}$, is

$$s^2 + \left[\frac{1}{3mCa_0}(k^4 - k^2) + \frac{2i}{m}\left(1 - \frac{1}{m}\right)N_B\right]s - i\frac{M_0}{m^2}k^3 = 0. \tag{25}$$

The solution to (25) is given by

$$s = \frac{1}{6mCa_0}(k^2 - k^4) - \frac{i}{m}\left(1 - \frac{1}{m}\right)N_B(k) \pm \frac{1}{2}\sqrt{\left[\frac{1}{3mCa_0}(k^4 - k^2) + \frac{2i}{m}\left(1 - \frac{1}{m}\right)N_B(k)\right]^2 + \frac{4}{m^2}ik^3M_0}, \tag{26}$$

which admits two roots of s. For a given set of parameters, we are interested in the most unstable mode whose s has the largest real part. In the absence of surfactant ($M_0 = 0$), Eq. (26) agrees with the linear stability result of Papageorgiou *et al.*,[7] and the core contribution to the instability is merely dispersive. In view of the fact that (26) contains the term $4ik^3M_0/m^2$ inside the square root, surfactant generally makes the system more unstable than the surfactant-free case. When viscosities of both fluids are matched ($m = 1$), the core dynamics are absent and the system's instability is solely determined by the film. The long wavelength ($k \to 0$) expansion of (26) with $m = 1$ yields

$$s = \pm\frac{1}{\sqrt{2}}i^{1/2}M_0^{1/2}k^{3/2} + O(k^2), \tag{27}$$

indicating that surfactant destabilizes the system for long waves. The leading order growth rates for long waves are $O(k^{3/2})$ due to Marangoni effects, and capillarity (due to its circumferential component) does not contribute to the instability until $O(k^2)$. The form of (27) is also identical to the $m = 1$ result of Wei and Rumschitzki[13] in spite of different scalings applied in their study. This is not unexpected because the instability of both systems is film-determined and Marangoni effects dominate for long waves. It is also consistent with the $m = 1$ result of Frenkel and Halpern[16] for the planar system with a semi-infinite upper layer.

The mechanism of the flow-induced Marangoni destabilization has been elucidated by the previous studies.[13,16] For completeness, below we choose the $m = 1$ case (in which the core dynamics are absent) for illustrating the instability mechanism. Consider the film flow region with a sinusoidal interfacial disturbance. As indicated by (21), the term $2\eta_z/m$ due to the perturbed basic interfacial velocity causes higher (lower) surfactant concentrations for the $\eta_z > 0$ ($\eta_z < 0$) portions of the interface. Such a perturbed surfactant distribution has maxima–minima at the interface nodes ($\eta = 0$), but has no changes at the interface crests/troughs ($\eta_z = 0$). That is, the surfactant distribution has a phase difference $\pi/2$ with the interface. The resulting Marangoni stresses in turn create flows from the interface nodes toward the crests/troughs, causing the interface to grow. Such Marangoni destabilization works for all $k(\ll\varepsilon^{-1})$, but is compromised by the short-wave capillary stabilization.

For $m \neq 1$ how surfactant interacts with viscosity strati-

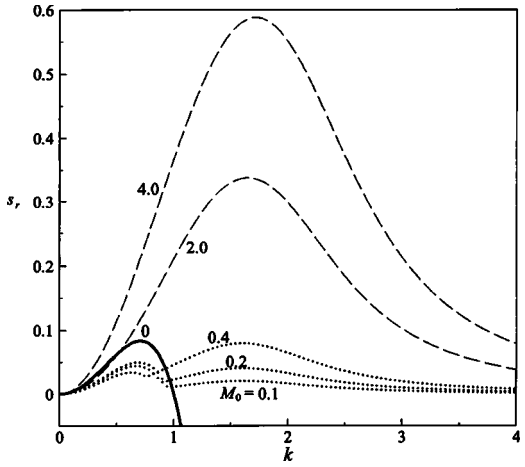

FIG. 2. The Marangoni effect on the growth rate curves for the Stokes flow case. $m=1.5$, $Ca_0=1$.

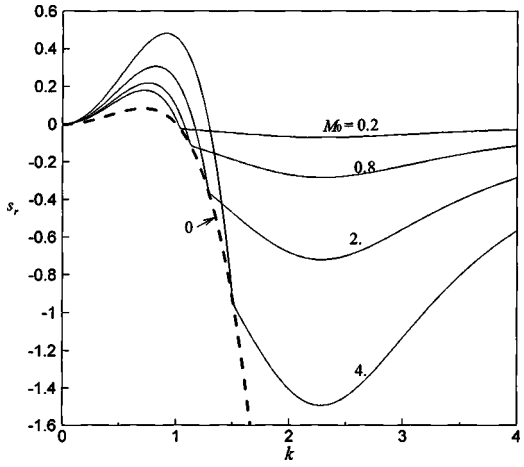

FIG. 3. The Marangoni effect on the growth rate curves for the Stokes flow case. $m=0.5$, $Ca_0=1$.

fication via coupling to the core flow becomes complicated. Figure 2 shows the s_r-k curves with $Ca_0=1$ and $m=1.5>1$ for various M_0. For $m>1$, in comparison with the $M_0=0$ case, adding surfactant makes the system unstable for all k ($\ll\varepsilon^{-1}$). Although the stabilizing effect of the axial capillarity slows down the growth rates for short waves, it does not make the growth rates negative. Increasing M_0 magnifies the destabilization. Note that M_0 here is restricted to $O(1)$ for ensuring $Ma=\varepsilon^2 M_0=O(\varepsilon^2)$ to retain the core coupling in view of (14).

The corresponding growth rate curves for the case of $m=0.5<1$ are shown in Fig. 3. The system with surfactant is more unstable than the surfactant-free case. There is a nonsmooth change in a growth rate, indicating that two eigenmodes switch their dominance in a range of k. Increasing M_0 promotes the longwave capillary destabilization while it suppresses the shortwave capillary stabilization. Since the shortwave capillary stabilization is mediated by the Marangoni destabilization, increasing M_0 shifts the critical wavelength toward a shorter one.

The long wavelength analysis may provide some insights into the above observations. For $m\neq 1$, in the limit of $k\to 0$, with the aid of $N_B=2k+\frac{1}{6}k^3+O(k^5)$, two roots of (26) become

$$s=\frac{M_0}{4(m-1)}k^2+O(k^3), \tag{28a}$$

$$s=-\frac{4i}{m}\left(1-\frac{1}{m}\right)k+\left[\frac{1}{3mCa_0}-\frac{M_0}{4(m-1)}\right]k^2+O(k^3). \tag{28b}$$

In contrast to (27) for the $m=1$ case whose longwave growth rates are $O(k^{3/2})$, the combined effects of surfactant and viscosity stratification on the long wavelength instability occurs at $O(k^2)$. This ordering is also consistent with the $m\neq 1$ result of Frenkel and Halpern.[16] The first mode (28a) involves the Marangoni-viscosity-stratification effect while the second (28b) further includes the usual $O(k^2)$ destabilization of the circumferential capillarity. The first mode is destabilizing (stabilizing) for $m>1$ ($m<1$). The second mode can destabilize the system for $m>1$ if $M_0Ca_0<\frac{4}{3}(1-1/m)$, and is always unstable for $m<1$. In the limit of $Ca_0\to\infty$ (i.e., $Ca_0\gg\varepsilon$), the dominant growth rate of both modes for $m\neq 1$ is $s_r=M_0k^2/4|m-1|+O(k^3)$, indicating that the large-Ca system is always unstable for long waves.

B. The $Re_1=O(1)$ case

The leading order linear stability for $Re_1=O(1)$ is governed by Eqs. (21) and (24). It is determined by the following dispersion equation:

$$s^2+\left[\frac{1}{3mCa_0}(k^4-k^2)-\frac{i}{m}\left(1-\frac{1}{m}\right)N_K\right]s-i\frac{M_0}{m^2}k^3=0, \tag{29}$$

which has two solutions of s:

$$s=\frac{1}{6mCa_0}(k^2-k^4)+\frac{i}{2m}\left(1-\frac{1}{m}\right)N_K\pm\frac{1}{2}\sqrt{\left[\frac{1}{3mCa_0}(k^4-k^2)-\frac{i}{m}\left(1-\frac{1}{m}\right)N_K\right]^2+\frac{4}{m^2}ik^3M_0}. \tag{30}$$

It can be shown that the $Re_1\to 0$ limit of (30) recovers the Stokes flow case as in the previous subsection. Figure 4 demonstrates the effect of Re_1 on the growth rates with $m>1$. For small and moderate Re_1, the growth rate curves have

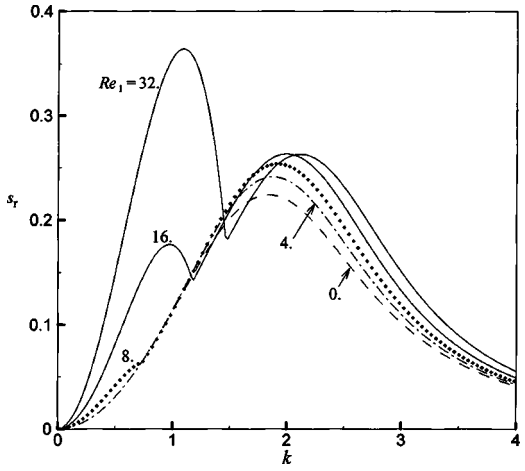

FIG. 4. The effect of Re_1 on the growth rates. $m=2$, $M_0=2$, $Ca_0=1$.

similar trends to those of Stokes flows, and increasing Re_1 makes slight increases in both the maximum growth rate $s_{r\,\max}$ and the corresponding wave number $k_{\max}$. For a large $Re_1(>8)$, however, the growth rate curve starts to exhibit an additional hump in a certain range of k. A nonsmooth transition between two humps indicates that two eigenmodes switch their dominance of the instability. As Re_1 increases, the first hump appearing in the smaller k regime starts to grow, but the second one in the larger k regime only slightly increases its maximum. The maximum of the first hump eventually becomes larger than the second at a sufficiently large Re_1 (that still satisfies $Re_1\varepsilon^3/m \ll 1$ for ensuring the validity of lubrication in the film).

For $m<1$, it is known that the core inertia acts to stabilize the system.[5] Adding surfactant could cause instability due to the flow-induced Marangoni effect. The stability arises from these two competing effects. Below we again utilize the long wavelength analysis to elucidate the combined effects of the core inertia and surfactant on the stability in more detail.

With the aid of $N_k=-4k-ik^2Re_1/12+O(k^3)$, two roots of (30) in the $k\to 0$ limit become

$$s=\frac{M_0}{4(m-1)}k^2+O(k^3), \tag{31a}$$

$$s=-\frac{4i}{m}\left(1-\frac{1}{m}\right)k+\left(\frac{1}{3mCa_0}-\frac{M_0}{4(m-1)}+\frac{1}{12m}\left(1-\frac{1}{m}\right)Re_1\right)k^2+O(k^3). \tag{31b}$$

In comparison with the $k\to 0$ asymptotics (28a) and (28b) of the $Re_1=O(\varepsilon)$ case, the first mode (31a) is identical to (28a), and is merely attributed to the Marangoni-viscosity-stratification effect that depends on neither Re_1 nor Ca. For the second mode (31b), it just adds the inertial correction to (28b). It is also clear from (31b) that the core inertia stabilizes (destabilizes) the system for $m<1$ ($m>1$). For $m<1$, the first mode is stabilized while the second mode is destabilized due to Marangoni effects. Therefore, for $m<1$ the instability is determined by the second mode (31b). There also exists a critical Reynolds number Re_1^* beyond which the instability is completely suppressed by the core inertia. In fact, Re_1^* can be estimated by setting the $O(k^2)$ part of (31b) to be zero:

$$Re_1^*\approx\frac{1}{\left(\frac{1}{m}-1\right)}\left(\frac{4}{Ca_0}+\frac{3M_0}{\left(\frac{1}{m}-1\right)}\right)\quad\text{for}\quad m<1. \tag{32}$$

Equation (32) suggests that surfactant destabilizes the $m<1$ system in a manner that Re_1^* increases with M_0. That is, the larger surfactant elasticity $El=MaCa$, the higher Re_1 required to stabilize the system. Table II lists the comparison between Re_1^* numerically evaluated by (30) and those using (32). The agreement is fairly good, indicating that (32) provides a lucid way to find Re_1^*.

TABLE II. The critical Reynolds number Re_1^* for various M_0. $m=0.5$, $Ca_0=1$.

M_0	Re_1^* from (30)	Re_1^* from (32)
0.0	4.00	4.00
0.2	4.45	4.60
0.5	5.35	5.50
1.0	6.85	7.00
2.0	9.85	10.0

VI. CONCLUDING REMARKS

We have asymptotically investigated the linear stability of a surfactant-laden CAF in the thin annular film ($\varepsilon\to 0$) limit. A scaling analysis is utilized to identify the dominant instability mechanisms in various parameter regimes. Rational scalings are established to examine the combined effects of Marangoni forces and viscosity stratification on the leading order linear stability of the system. For both cases in the absence and the presence of core inertia, the respective coupled sets of the linear stability evolution equations are derived for the interfacial deflection and the surfactant concentration.

For a core flow with negligible inertia, in contrast to the clean-interface case whose core dynamics do not contribute to the system's stability, the interaction between surfactant and the core flow can significantly affect the stability. When the film is more viscous, surfactant makes the system unstable for all disturbance wavelengths that are much longer than the annulus thickness. For the system with a more viscous core, surfactant promotes the longwave destabilization and the shortwave stabilization of capillarity.

In the case in the presence of the core inertia, the features of instability can be modified due to surfactant, especially for the system with a more viscous core. There exists a critical Reynolds number Re_1^* beyond which the instability is completely suppressed by the core inertia. Surfactant destabilizes the system in a manner that Re_1^* increases with surfactant elasticity.

Extension of the current linear stability analysis to the weakly nonlinear regime could be rather interesting. On the one hand, surfactant could induce more severe destabiliza-

tion than the clean-interface case; on the other hand, the instability could be arrested in the weakly nonlinear regime due to steepening interfacial deflections and to shortwave capillary stabilization. The fate of the interface seems to hinge on the competition between these effects, depending on the sizes of perturbations and the scales of all relevant parameters. For example, if the size of an interfacial perturbation has $\delta_1 \sim \varepsilon^2$ as in Papageorgiou *et al.*,[7] then the surfactant concentration could have a variation of $\delta_2 \sim O(1)$ according to our present analysis. This means that although the interfacial perturbation is confined within the small-amplitude regime, the surfactant concentration variation is large. A similar approach to Kerchman's[8] might provide more insights into all occurrences in this scenario.

Moreover, Papageorgiou *et al.*[7] demonstrated for clean-interface CAFF's that the interfacial dynamics derived from Kuramoto–Sivashinsky-type equations could exhibit travelling waves or chaotic motions. If the interfacial instability with surfactant can be indeed arrested in the weakly nonlinear regime, one may raise another question how surfactant modifies the spatio-temporal features of the nonlinear interfacial dynamics.

ACKNOWLEDGMENT

This research work was supported by the National Science Council of Taiwan under Grant No. NSC92-2218-E006-057.

[1] L. Preziosi, K. Chen, and D. D. Joseph, "Lubricated pipelining: Stability of core-annular flow," J. Fluid Mech. **201**, 323 (1989).
[2] C. W. Park and G. M. Homsy, "Two-phase displacement in Hele-Shaw cells: Theory," J. Fluid Mech. **141**, 257 (1984).
[3] T. Babadagli, "Selection of proper enhanced oil recovery fluid for efficient matrix recovery in fractured oil reservoirs," Colloids Surf., A **223**, 157 (2003).
[4] F. F. Espinosa and R. D. Kamm, "Bolus dispersal through the lungs in surfactant replacement therapy," J. Appl. Physiol. **86**, 391 (1999).
[5] E. C. Georgiou, D. T. Papageorgiou, C. Maldarelli, and D. S. Rumschitzki, "An asymptotic theory for the linear stability of a core-annular flow in the thin annular limit," J. Fluid Mech. **243**, 653 (1992).
[6] A. L. Frenkel, A. J. Babchin, B. G. Levich, T. Shlang, and G. I. Sivashinsky, "Annular flows can keep unstable film from breakup: Nonlinear saturation of capillary instability," J. Colloid Interface Sci. **115**, 225 (1987).
[7] D. T. Papageorgiou, C. Maldarelli, and D. S. Rumschitzki, "Nonlinear interfacial stability of core annular flows," Phys. Fluids A **2**, 340 (1990).
[8] V. Kerchman, "Strongly nonlinear interfacial dynamics in core-annular flows," J. Fluid Mech. **290**, 131 (1995).
[9] C. Kouris and J. Tsamopoulos, "Dynamics of axisymmetric core-annular flow in a straight tube. I. The more viscous fluid in the core, bamboo waves," Phys. Fluids **13**, 841 (2001).
[10] C. Kouris and J. Tsamopoulos, "Dynamics of the axisymmetric core-annular flow. II. The less viscous fluid in the core, saw tooth waves," Phys. Fluids **14**, 1011 (2002).
[11] R. Bai, K. Kelkar, and D. D. Joseph, "Direct simulation of interfacial waves in a high-viscosity-ratio and axisymmetric core-annular flow," J. Fluid Mech. **327**, 1 (1996).
[12] D. S. Rumschitzki, "The effect of insoluble surfactants on the linear stability of a core-annular flow," 2000 AIChE Annual Meeting, Los Angeles (2000).
[13] H.-H. Wei and D. S. Rumschitzki asympototically examined the effect of surfactant on the linear stability of a CAF in the thin-annulus limit. The leading order stability is governed by the annular film flow to which the core dynamics are slaved. The effect of surfactant on the stability lies in the interplay between capillarity Marangoni effects, and base flows. This work has been submitted to J. Fluid Mech. (to be published).
[14] K. J. Cassidy, D. Halpern, B. G. Ressler, and J. B. Grotberg, "Surfactant effects in model airway closure experiments," J. Appl. Physiol. **87**, 415 (1999).
[15] D. Halpern and J. B. Grotberg, "Nonlinear saturation of the Rayleigh instability in a liquid-lined tube due to oscillatory flow," J. Fluid Mech. **492**, 251 (2003).
[16] A. L. Frenkel and D. Halpern, "Stokes-flow instability due to interfacial surfactant," Phys. Fluids **14**, L45 (2002).
[17] D. Halpern and A. L. Frenkel, "Destabilization of a creeping flow by interfacial surfactant: Linear theory extended to all wavenumbers," J. Fluid Mech. **485**, 191 (2003).
[18] H. Wong, D. Rumschitzki, and C. Maldarelli, "On the surfactant mass balance at a deforming fluid interface," Phys. Fluids **8**, 3203 (1996).
[19] H. Chen, L. Han, P. Luo, and Z. Ye, "The interfacial tension between oil and gemini surfactant solution," Surf. Sci. Lett. **552**, L53 (2004).